Lithuanian Journal of Physics, Vol. **52,** No. 1, pp. 24–29 (2012)

SURFACE-FRACTURE-RELATED PHOTOLUMINESCENCE OF CdMnTe CRYSTALS

R. Brazis [a], A. Selskis [a], B. Kukliński [b], and M. Grinberg [b]

[a] *Centre for Physical Sciences and Technology, A. Goštauto 11, LT-01108 Vilnius, Lithuania*
E-mail: brazis@pfi.lt; aselskis@ktl.mii.lt
[b] *Experimental Physics Institute of the University of Gdańsk, Wita Stwosza 57, 80-952 Gdańsk, Poland*
E-mail: fizmgr@univ.gda.pl

Received 29 August 2011; revised 28 February 2011; accepted 1 March 2011

Enhanced photoluminescence from sub-wavelength crystallites attached to the fractured surface of cleaved host crystals, and the transfer of emitted light to the dark side of macroscopically thick absorbing samples of $Cd_{1-x}Mn_xTe$ with $x = 0.2$ is reported. The conventional model based on Kirchhoff's law of radiation is found to fail to describe the experimental photoluminescence line and its red shift relative to the optical absorption, and a more adequate novel theoretical model implying population inversion is proposed.

Keywords: CdMnTe, photoluminescence, optical absorption, electron microscopy, nanoparticles

PACS*:* 78.40.Fy, 78.20.Ci, 78.55.Et, 78.67.Bf

1. Introduction

$Cd_{1-x}Mn_xTe$ solid solutions have been primarily synthesised for experimental verification of the concept of exchange interaction of Mn magnetic moments with electron and hole spins [1-7]. The discovery of giant Faraday rotation in these crystals invoked magnetooptical device engineering [8-12]. It triggered research in low-dimensional structures with magnetic ions [13-15] for nanophotonics and spintronics [16]. Besides magnetic interaction, cadmium substitution just by smaller-size Mn atoms brings about the crystal lattice contraction allowing for graded band-gap structure engineering for photoelectronic devices. Mn-related bands of high-energy photon absorption in $Cd_{1-x}Mn_xTe$ also find applications in X- and γ-ray detectors [17].

One of the basic crystal parameters determining the spectral range of applications is the energy gap E_g between the valence band top and conduction band bottom. As the lattice constant decreases nearly linearly, a/nm = 0.647–0.0133x [18], E_g is nearly linearly increasing with the Mn molar contents x. Attempts to deduce $E_g(x)$ from the optical absorption (OA) or photoluminescence (PL) spectral measurements indeed reveal nearly linear behaviour for $x < 0.4$. Above this value, PL line branch appears at 2 eV, independent of x, which is related to transitions between the excited and ground states of Mn ions [5, 19-23]. OA measurements also show $E_g(x)$ tending to saturate for $x > 0.4$, but at somewhat higher level of 2.15–2.25 eV, depending on lattice temperature [12]. At any value of x, the values of $E_g(x)$ deduced from OA and PL turn out to be different, and the origin of this difference is not clear.

OA coefficient $\alpha(h\nu)$ measured as a function of photon energy $h\nu$ at the low-energy tail of the fundamental absorption edge is analysed conventionally using Urbach's rule and Varshni formula [24], and E_g is extracted as one of the five adjustable parameters depending on the Mn contents. Some of the adjustable parameters are formal, e. g. the "phonon energy", which needs to be about twice as high as the highest-energy phonon mode in these materials: LO phonon energy is about 24 meV in CdTe, and it does not change much with the rise of Mn contents [25].

Energy gap determination seems to be more reliable when the exciton-related peak of the absorption coefficient is resolved [26]. Nevertheless, the "true" energy gap value remains questionable as the OA tail and OA peak measurements give different E_g values and the PL peak is red-shifted relative to that of OA.

The shift of the PL peak has been explained recently by the inverted population of states in a matter spatially confined to the sub-wavelength scale [27-29]. The self-organised confinement of light emitters to nanometre-scale clusters in the $Cd_{1-x}Mn_xTe$ bulk was deduced earlier from the analysis of composition disorder and magnetic fluctuations [30].

This article reports on experimental observation of new effects in light interaction with $Cd_{1-x}Mn_xTe$ crystals: PL enhancement by sub-wavelength crystallites attached to the fractured surface of cleaved host crystals, and the transfer of emitted light to the dark side of macroscopically thick absorbing samples of $Cd_{1-x}Mn_xTe$ with $x = 0.2$. Theoretical PL line models and conclusions are presented below.

2. Experiment

$Cd_{1-x}Mn_xTe$ crystals grown by the Bridgeman method with $x = 0.2$ were selected in order to have band-gap PL below the Mn atomic-level luminescence line (being at 2 eV). Samples were prepared for PL measurements by cleaving in order to get optically perfect surface area. However, at the cleaving instant, numerous different-size crystallites are produced attaching to the surface by electrostatic and magnetic forces (Fig. 1).

The smallest resolvable crystallite size is about 10 nm, and the largest crystallites observed are up to 1 μm size. At this piloting stage of the experiment, we have omitted the specification of a particular crystallite responsible for emission. We observed bright light outbursts when scanning manually the samples by the Ar laser beam. Focusing the beam allowed to select visually a single star-like emitter and to record its spectrum (Fig. 2).

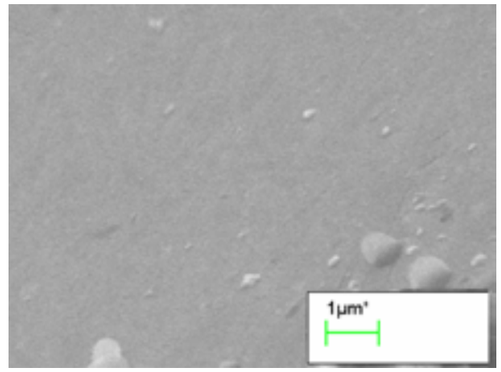

Fig. 1. View on the surface of cleaved $Cd_{1-x}Mn_xTe$ crystal ($x = 0.2$) by ZEISS scanning electron microscope EVO 50.

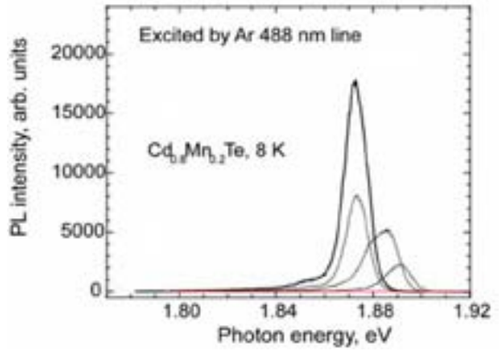

Fig. 2. PL of $Cd_{1-x}Mn_xTe$ ($x = 0.2$) excited by the 488 nm line of Ar laser at $T = 8$ K at different points on the surface. The line peaked at 1.89 eV is recorded from the apparently crystallite-free area.

The crystallite PL peak positions are red-shifted relative to the peak of fundamental absorption (being at 1.91 eV for this particular Mn mole fraction $x = 0.2$ [31]).

3. Theory

The modelling of PL spectral distribution is conventionally addressed to van Roosbroeck and Shockley who published their theory of recombination radiation balanced in details with the light absorption in crystals [32]. In this model, radiation intensity is

$$I(E) = Dn^3\kappa \frac{E^3}{\exp[E/(k_B T_{ef})]-1}. \quad (1)$$

Here E is the photon energy, D is the apparatus-related constant, n is the refraction index, κ is the absorption index, k_B is the Boltzmann constant, and T_{ef} is the effective temperature that not necessarily equals that of the crystal lattice. In other recipes (named after Stepanov or Kennard-Stepanov [33], or Kubo-Martin-Schwinger [34, 35]) the Plank's factor $1/\{\exp[E/(k_B T_{ef})]-1\}$ in Eq. (1) is replaced by the Boltzmann or other universal function $f(E, T)$. All the approaches rely basically on Kirchhoff's law of thermal-equilibrium radiation, except for the explicit form of the universal function $f(E, T)$.

Figure 3 illustrates the result of intensity calculation using Eq. (1) with the values of $n(E)$ and $\kappa(E)$ for $Cd_{0.8}Mn_{0.2}Te$ as given by the complex dielectric function $\varepsilon(E)$ deduced from reflectivity measurements in Ref. [31], supposing the effective temperature to be T_{ef} = 400 K. The adjustable effective temperature is conventionally attributed to the light-emitting ensemble (excitons, electron-hole gas, etc.); therefore, it is set high compared to the crystal lattice temperature. The choice of T_{ef}, which enters the Planck's factor only, affects the intensity spectrum slope and magnitude, and the peak position is determined by the dispersion of the refraction and absorption coefficients. As is seen in Fig. 3, this theory does not model the experimental PL line shape: the theoretical intensity maximum is practically at the position of maximum absorption, whereas the experimental PL peak is significantly red-shifted.

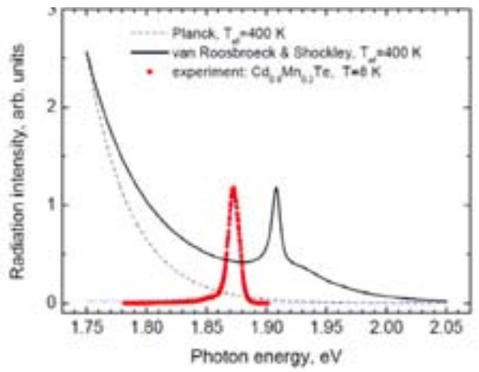

Fig. 3. Light emission spectrum calculated by the van Roosbroeck-Shockley model (Eq. (1)) with T_{ef} = 400 K for the refraction and absorption indexes $n(E)$ and $\kappa(E)$ of $Cd_{0.8}Mn_{0.2}Te$ determined from Ref. [31] (solid line), compared with the experimental PL spectrum for $Cd_{0.8}Mn_{0.2}Te$ excited by the 488 nm line of Ar laser at T = 8 K (dots), and the blackbody radiation spectrum for T = 400 K (dashed line).

Further we will turn to an alternative concept [27-29]. Suppose that the particles interacting with light can be in two allowed states only: the ground one with the energy E_l and zero dipole moment, and the excited one with the energy E_m and a finite dipole moment. For the light energy absorption, the light-induced change of dipole moment needs to be *in phase* with the light electric field, whereas the acts of energy emission need the dipole moment change to be *in opposite phase* to the light electric field. The Schrödinger equation solution for perturbation by time-dependent electric field results in the oscillator-like contributions to the dielectric function,

$$\varepsilon(E) = \varepsilon_\infty(E) + \frac{\beta^2_{lm} N_l}{[(E_m - E_l)^2 - (E)^2] + iE\Gamma_{lm}} - \frac{\beta^2_{ml} N_m}{[(E_m - E_l)^2 - (E)^2] + iE\Gamma_{ml}}, \quad (2)$$

where $\varepsilon_\infty(E)$ is the background dielectric function, Γ_{lm} is the joint level broadening parameter, and β^2_{lm} is the coefficient controlled by the square matrix element of the dipole moment operator for the l-m transition. The values of Γ_{ml} and β^2_{ml} for m-l transitions are here supposed to be the same as for *l-m* transitions, and N_l and N_m are the occupation numbers of the ground and excited levels.

Let the light absorbing/emitting matter be bounded in a sub-wavelength-size spheroid surrounded by a dielectric medium. A quasi-static approximation can be then used for finding the spheroid electric and magnetic moments [36]. The power absorbed or emitted by the spheroid electric dipole perturbation is [37]

$$P = \frac{1}{2}\frac{E}{\hbar}\varepsilon_0\varepsilon_M V\left(\frac{1}{L}\right)^2 \times \frac{\mathrm{Im}\varepsilon(E)}{[\mathrm{Re}\varepsilon(E) + \varepsilon_M\gamma_L]^2 + [\mathrm{Im}\varepsilon(E)]^2}|E_0|^2. \quad (3)$$

Here ε_M is the dielectric constant of matrix surrounding the spheroid, V is the spheroid volume, L is its depolarisation factor (e. g. L = 1/3 for the sphere), $\gamma_L = (1/L) - 1$, E_0 is the light wave electric field amplitude in the matrix. The matrix dielectric constant ε_M is not well defined for crystallites being at the air/crystal interface. The crystallite depolarisation factor is generally tensor [38 and its values can be influenced by the crystallite image in the host crystal. A similar complexity of factors has been considered by Berreman in his theory [39] of infrared radiation scattering on the rough surface of ionic crystals. The pits and bumps at the surface in that model have been concluded to act as sub-wavelength spheroids with the fractional values of γ_L giving rise to resonant distortions in the Reststrahl band.

By adapting these concepts for the visible light interaction with electronic oscillators, we compare here two simple cases of a spheroid being in air and that embedded in the host matrix. We take again the complex dielectric function $\varepsilon(E)$ of $Cd_{0.8}Mn_{0.2}Te$ as deduced from reflectivity measurements in Ref. [31] keeping the background component independent of whether the crystal is in normal or in excited state and inverting sign (when modelling emission) of the component of inter-band transitions. This model gives the PL line shape and peak position in good agreement with the experiment (Fig. 4).

Although Fig. 4 presents calculations for the particular (50 nm) size spheroid, the peak position according to Eq. (3) should remain insensitive to the size change as far as the spheroid remains essentially smaller than the light wavelength. Some variation of the peak positions can arise depending on the crystallite shape due to shape-dependent depolarisation factors. The crystallite size, i. e. the amount of light-emitting matter, controls the peak height. The calculated PL spectra have smaller widths compared to the experimentally obtained spectrum, and this question remains for future analysis including both the homogeneous and inhomogeneous broadening contributions.

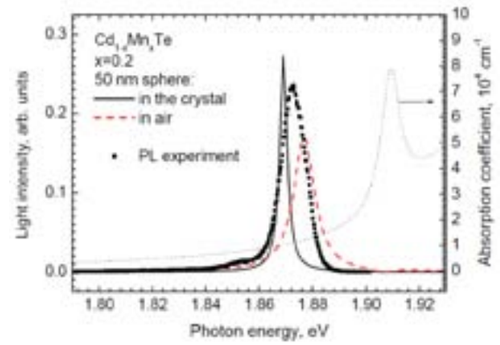

Fig. 4. Experimental PL intensity from a $Cd_{0.8}Mn_{0.2}Te$ crystallite on the cleaved host crystal surface (squares) and light intensity calculated for the excited state of $Cd_{0.8}Mn_{0.2}Te$ sphere suspended in air (dashed line) and in the host crystal (solid line). The absorption coefficient for $Cd_{0.8}Mn_{0.2}Te$ from Ref. [31] is included for comparison (dotted line).

As is seen in Eq. (3), for sufficiently small level broadening $\Gamma_{lm} \to 0$) and transparent matrix ($\varepsilon_M > 0$), the power absorption/emission is peaked at the condition of Re $\varepsilon(E) = -\varepsilon_M \gamma_L$ that requires the value of Re $\varepsilon(E)$ to be negative. For the normal population ($N_l > N_m$) the resonance (peak absorption) takes place at the photon energy *higher* than the inter-level distance: $E_{OA} > E_m - E_l$. For the inverse population, the resonance (peak emission) takes the place at a *lower* energy side: $E_{PL} < E_m - E_l$, i. e. The PL peak is red-shifted relative to that of absorption. Taking for absorption the population numbers of N_l = 1, N_m = 0, and for emission the values of N_l = 0, N_m = 1, respectively, and tending $\Gamma_{lm} \to 0$, one gets from Eq. (2) the value of Re $\varepsilon(E) = \varepsilon_\infty \pm \beta^2 / [(E_m - E_l)^2 - E^2]$ where (+) stands for the process of OA, and (–) for PL. With the condition of Re $\varepsilon(E) = \varepsilon_M\gamma_L$ this gives

$$E_m - E_l = \sqrt{(E^2_{OA} + E^2_{PL})/2}, \quad (4)$$

and the red shift, which is-

$$\Delta = E_{OA} - E_{PL} = \beta^2 / \left[(\varepsilon_\infty + \varepsilon_M\gamma_L)\sqrt{(E^2_{OA} + E^2_{PL})/2}\right]. \quad (5)$$

Although the band-gap $E_g \equiv E_m - E_l$ and the red shift Δ evaluation require complementary experiments on absorption in crystallites instead of absorption spectrum of the bulk crystal[1], it is interesting to make at this stage tentative estimations based on Eqs. (4) and (5). Experimental OA and PL peak positions give the red shift, which is $\Delta \approx 31$ meV, and the oscillator strength measure for the conduction-valence-band transitions; it is $\beta^2_{cv} = (0.88\pm0.34)$ eV^2, with the large error bar due to the uncertainty of $\varepsilon_M \gamma_L$ values. The band-gap value for CdMnTe with Mn mole contents $x = 0.2$ is then $E_g \approx \sqrt{(E^2_{OA} + E^2_{PL})/2} \approx 1.89$ eV.

4. Dark side lighting

Unexpected bright photoluminescence appeared also on the dark side of approximately 1-mm- thick crystal. The absorption coefficient at the position of the PL peak is of the order of 1×10^4 cm^{-1} (Fig. 4) ruling out the conventional transmission of light from the illuminated one to the dark side. It is likely that energy transfer to the dark side is mediated by magnetically interacting Mn^{2+} ions.

5. Conclusion

The scanning electron microscopy of the cleaved $Cd_{0.8}Mn_{0.2}Te$ crystals revealed multiple crystallites created at the crystal cleaving instant. The crystallites are quite tightly bound to the surface by electrostatic and magnetic forces. The SEM-resolvable crystallite size ranged to 10 nm. The scanning of the fractured surface with the Ar laser beam revealed the crystallites giving bright photoluminescence. The theory by van Roosbroeck and Shockley [32] based on Kirchhoff's law of radiation, which is conventionally used in the PL line analysis, does not describe the red shift of PL relative to OA. The red shift, which is the most common feature in experimental PL observations, is in reasonable agreement with calculations based on the model suggested by Brazis [27-29] taking into account normal/inverted states of the sub-wavelength emitters/absorbers. The enhanced light emission and absorption by the fractured surface and particularly unexpected bright photoluminescence observed on the dark side of $Cd_{0.8}Mn_{0.2}Te$ crystals are encouraging features for experimental research continuation aiming at a more controllable technology. The dark-side lighting relation to Mn^{2+} challenges for experimental research in the whole range of Mn molar contents. In the more Mn-reach structures, the theoretical model will also need to take into account internal optical transitions in Mn^{2+} competing with the transitions between the valence and conduction bands.

1 OA peak position for $Cd_{0.8}Mn_{0.2}Te$, as shown in Fig. 4, has been determined in earlier experiments [31].

Acknowledgments

One of the authors (R. B.) acknowledges support by the EU COST Action MP0702 and the Research Counsil of Lithuanian (grant #KEL-202/2011) for the research presentation at international conferences.

References

[1] N.T. Khoi and J.A. Gaj, Phys. Status Solidi B **83**, K133 (1977).
[2] A.V. Komarov, S.M. Ryabchenko, O.V. Terletskii, I.I. Zheru, and R.D. Ivanchuk, J. Exp. Theor. Phys. **73**, 608 (1977) [in Russian].
[3] J.A. Gaj, R.R. Gałązka, and M. Nawrocki, Solid State Commun. **25**, 193 (1978).
[4] R.A. Abreu, J. Stankiewicz, and W. Giriat, Phys. Status Solidi A **75**, K153 (1980).
[5] R.R. Gałązka, S. Nagata, and P.H. Keesom, Phys. Rev. B **22**, 3344 (1980).
[6] J.K. Furdyna, J. Appl. Phys. **53**, 7637 (1982).
[7] J.K. Furdyna, J. Appl. Phys. **64**, R29 (1988).
[8] K. Morimoto, K. Takagi, and K. Matsubara, United States Patent 4789500, issued 12.06.1988.
[9] Y. Tomita, H. Oda, and M. Okuda, United States Patent 5245465, issued 09.14.1993.
[10] M. Yamanishi and H. Oda, Patent Document Number CA 2036759 C, issued 26.07.1994, Canadian Patent Database.
[11] V. Zayets, M.C. Debnath, and K. Ando, Appl. Phys. Lett. **84**, 565 (2004).
[12] Y. Hwang, S.-S. Chung, and Y. Um, Phys. Status Solidi C **4**, 4453 (2007).
[13] J.A. Gaj, in: *Semiconductors and Semimetals*, Vol. 25 (Academic Press Inc., New York, 1992) pp. 296–331.
[14] R. Brazis, R. Narkowicz, L. Safonova, and T. Wojtowicz, in: *Optical Properties of Semiconductor Nanostructures*, eds. M.L. Sadowski, M. Potemski, and M. Grynberg, NATO Sci. Ser. 3 – High Technol. **81**, 315 (2000).
[15] W. Dobrowolski, J. Kossut, and T. Story, *Handbook of Magnetic Materials*, Vol. 15, ed. K.H.J. Bushow (Elsevier Science B.V., Amsterdam, 2006) pp. 298–378.

[16] T. Dietl, Nat. Mater. **9**, 965 (2010).
[17] A. Hossain, Y. Cui, A.E. Bolotnikov, G.S. Camarda, G. Yang, D. Kochanowska, M Witkowska-Baran, A. Mycielski, and R.B. James, J. Electron. Mater. **38**, 1593 (2009).
[18] A. Balzarotti, N. Motta, A. Kisiel, M. Zimnal-Starnawska, M.T. Czyżyk, and M. Podgórny, Phys. Rev. B **31**, 7526 (1985).
[19] M.P. Vecchi, W. Giriat, and L. Videla, Appl. Phys. Lett. **38**, 99 (1981).
[20] M.M. Moriwaki, W.M. Becker, W. Gebhardt, and R.R. Galazka, Phys. Rev. B **26**, 3165 (1982).
[21] E. Müller and W. Gebhardt, Journal of Luminescence, **31–32**, 479 (1984).
[22] D. Leinen, Phys. Rev. B **55**, 6975 (1997).
[23] Y. Hwan, Y. Um, and H. Park, J. Korean Phys. Soc. **58**, 1312 (2011).
[24] Y. Hwang, Y. Um, and H. Kim, J. Korean Phys. Soc. **34** 405 (1999).
[25] S. Venugopalan, A. Petrou, R.R. Gałązka, A.K. Ramdas, and S. Rodriguez, Phys. Rev. B **25**, 2681 (1982).
[26] I. Caraman, G.I. Rusu, and L. Leontie, J. Optoelectron Adv. Mater. **8**, 107 (2006).
[27] R. Brazis, in: *COST MP0702 Managing Committee and Working Group Meeting "Towards Functional Sub-Wavelength Photonic Structures"* (International Laser Center of Bratislava, Slovak Republic, 26–28 Oct 2008) p. 22.
[28] R. Brazis, in: *12th ICTON*, 27 June–1 July 2010, Munich, Germany, Conf. Proc. (IEEE 2010 online) p. 4.
[29] R. Brazis, in: *13th ICTON*, 26–30 June 2011, Stockholm, Sweden, Conf. Proc. (IEEE 2011 online) p. 4.
[30] R. Brazis and J. Kossut, Solid State Commun. **122**, 73 (2002).
[31] L. Safonova, R. Brazis, and R. Narkowicz, Lith. J. Phys. **44**, 421 (2004).
[32] W. van Roosbroeck and W. Shockley, Phys Rev. **94**, 1558 (1954).
[33] B.I. Stepanov, Dokl. Akad. Nauk BSSR **112**, 839 [in Russian, English translation in: *Doklady Sov. Phys.* **2**, 81 (1957)].
[34] R. Kubo, J. Phys. Soc. Jpn. **12**, 570 (1957).
[35] P.C. Martin and J. Schwinger, Phys. Rev. **115**, 1342 (1959).
[36] R.S. Brazis and J.K. Furdyna, Phys. Rev. B **16**, 3273 (1977).
[37] R.S. Brazis, J.K. Furdyna, and J.K. Požela, Phys. Status Solidi A **54**, 11 (1979).
[38] L.D. Landau, E.M. Lifshitz, *Electrodynamics of Continuous Media* (Moscow, 1959) pp. 42–43 [in Russian].
[39] D.W. Berreman, Phys. Rev. **163**, 85 (1967).

SKELTO PAVIRŠIAUS SĄLYGOTA CdMnTe KRISTALŲ FOTOLIUMINESCENCIJA

R. Brazis [a], A. Selskis [a], B. Kukliński [b], M. Grinberg [b]

[a] *Fizinių ir technologijos mokslų centras, Vilnius, Lietuva*

[b] *Gdansko universiteto Eksperimentinės fizikos institutas, Gdanskas, Lenkija*

Santrauka

Eksperimentiškai tiriant skelto $Cd_{1-x}Mn_xTe$ ($x = 0,2$) monokristalo paviršiaus fotoliuminescenciją nustatyta, kad švytėjimas sustiprėja kiekvieną kartą, kai žadinantis Ar lazerio spindulys nutaikomas į kurį nors iš aibės kristalitų, kuriais paviršius pasidengia skaldymo metu. Ryškus švytėjimas aptiktas ir tamsiojoje (nesužadintoje) pusėje, šviesai praėjus per storą neskaidrų kristalą. Elektroniniu mikroskopu paviršiuje buvo pastebėti kristalitai didesni už dešimtį nanometrų. Parodyta, kad įprastinis fotoliuminescencijos modelis, pagrįstas Kirchhoff'o spinduliavimo dėsniu, neaprašo eksperimentinio spektro smailės raudonojo poslinkio nuo sugerties smailės. Eksperimentą paaiškina naujas modelis, grindžiamas dviejų lygmenų normalios ir apgrąžos užpildos teorija.